

# Response of three Athens metro underground structures in the 1999 Parnitha earthquake

G. Gazetas\*, N. Gerolymos, I. Anastasopoulos

*School of Civil Engineering, Geotechnical Engineering Division, National Technical University, Athens, Greece*

Accepted 1 November 2004

## Abstract

The  $M_s$  5.9 earthquake of 1999 produced valuable records in three underground structures, as follows: (a) in the just completed cut-and-cover station of Sepolia two accelerographs recorded the free-field and the station-base motion; (b) in the still under-construction tunnelled station of Monastiraki an accelerograph recorded the ground surface motion, and (c) in the nearby Kerameikos station, abandoned for non-technical reasons, the temporary prestressed-anchor piled (PAP) wall was still in place and produced a record of total seismic displacement at its top. Directly or indirectly utilising these records, the article outlines the results of numerical analyses aimed at ‘recovering’ the complete seismic response of the three underground structures. Particular emphasis is given to Sepolia station, where the developed accelerations (with PGA of about 0.17 g at the station base and 0.43 g at the station roof) are shown to have been almost exactly equal to the design accelerations according to the seismic code under the assumption that the station responds as an aboveground structure. The successful performance of the two temporary structures, in Monastiraki and Kerameikos (which had been designed against minimal acceleration levels but experienced ground-surface high-frequency accelerations of the order of 0.50 g) is explained through dynamic response analyses.

© 2005 Elsevier Ltd. All rights reserved.

*Keywords:* Cut-and-cover station; Anchored pile wall; Seismic response; Seismic observation; Seismic analysis; Earth pressures; Underground structures; Soil–tunnel interaction

## 1. Introduction

The  $M_s$  5.9 Parnitha (Athens) Earthquake occurred at a time when the two lines of the new Metro of Athens were in the final stage of completion. Fortunately, just a few months earlier, 10 accelerographs had been installed in a number of subway stations and on the ground surface. These were triggered in the 7 September 1999 event, and provided valuable records of ground motions and of the response of underground stations. In some unfinished structures, continuous monitoring of stresses and deformations also provided useful data.

Particularly interesting were the records of the response of the following three underground structures: (a) the still under-construction tunnelled station of Monastiraki, where an accelerograph recorded the ground surface motion,

(b) the finished cut-and-cover station of Sepolia, where two accelerographs recorded the free-field and the station-base motion; and (c) the Kerameikos station, abandoned for non-technical reasons, where the 23 m-high temporary prestressed-anchor piled (PAP) wall was still in place and produced a record of seismic displacement at its top.

Directly or indirectly utilising these records, the article outlines the results of numerical analyses aimed at ‘recovering’ the seismic response of the three underground structures. Particular emphasis is given to the Sepolia station which experienced accelerations with peak values of about 0.18 g at the station base and 0.45 g at the station roof—almost exactly equal to the design accelerations. Still, the largest bending moments are shown to be inferior to the ultimate capacity of the reinforced-concrete structure by a rather substantial margin. The successful performance of the two temporary structures, in Monastiraki and Kerameikos, which had been designed against minimal (or zero) acceleration levels but experienced ground-surface accelerations of the order of 0.50 g, is explained through dynamic response analyses.

\* Corresponding author. Tel.: +30 210 772 3435.

**2. The 1999 Parnitha (Athens) earthquake**

The  $M_s$  5.9 Parnitha earthquake of September 7, 1999, ruptured an unmapped blind normal fault, the surface projection of which is portrayed in Fig. 1. Detailed information on seismological, geological and engineering aspects of the earthquake can be found in [1–3].

The fault-plane solutions of the mainshock and the spatial distribution of aftershocks suggest that the rupture originated at a depth of about 12 km and propagated *upward* and *eastward*, with the number of aftershocks being greater in the eastern part of the fault, i.e. the part closer to Athens. One would therefore, expect *forward-directivity* effects to

have been present in the ground motions experienced at sites located to the east of the rupture zone, at distances within a few kilometres. Indeed, that is, where the damage was concentrated.

The structural damage was extensive in the NNW part of the Athens metropolitan region: about 80 residential and industrial buildings collapsed, and more than 1500 buildings were damaged ‘beyond repair’. *Repairable* damage was far more widespread over a metropolitan region with about 1.5 million inhabitants. More significantly, 145 people died under the ruins of 30 buildings. This constitutes the third largest casualty figure for an earthquake in Greece in the 20th century. The location of these buildings is depicted in Fig. 1.

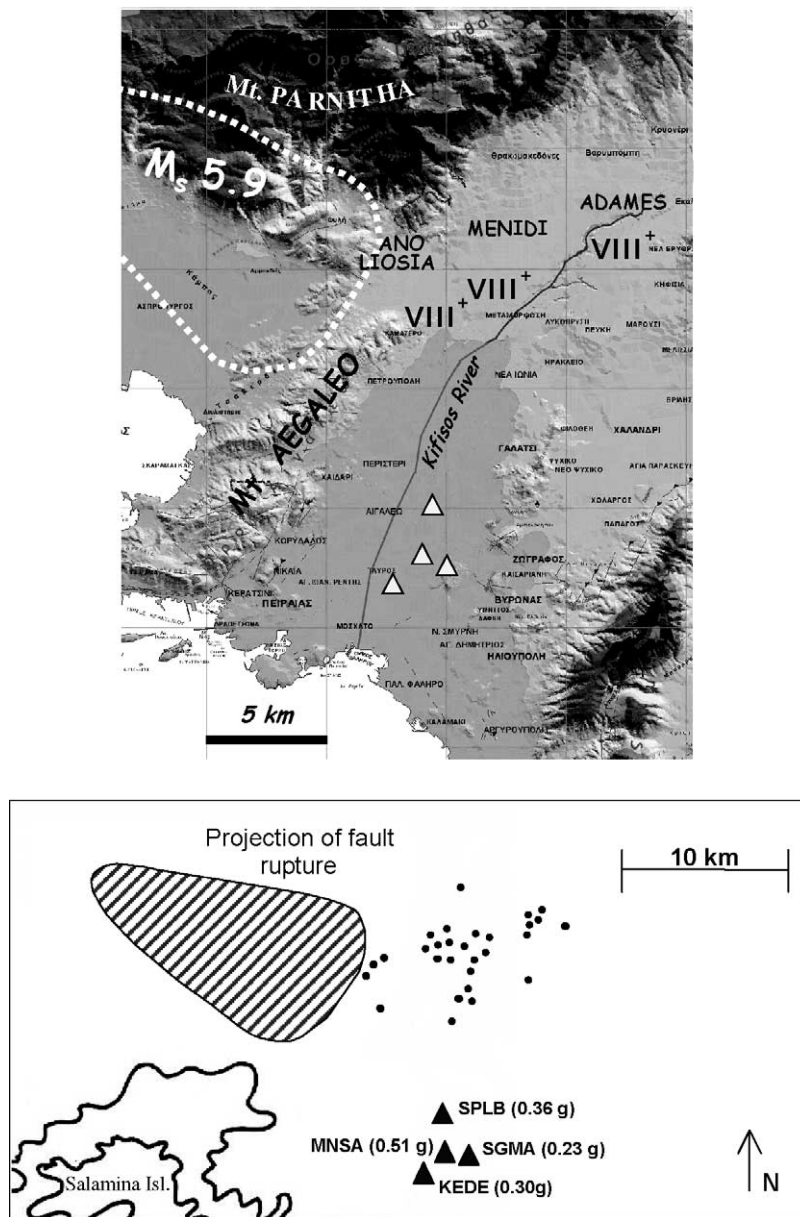


Fig. 1. Map of the earthquake stricken region showing the surface projection of the fault. Most of the accelerograph stations (triangles) were close to the city-centre. The circles show the exact location of the 30 collapsed buildings with human casualties. (Adapted from Gazetas [3]).

Fifteen strong-motion accelerograph stations were triggered by the main shock within 25 km from the fault. Peak ground accelerations (PGA) ranging from about 0.05 g up to 0.51 g were recorded. Fig. 1 shows the location of the most important accelerograph stations. Emphasis is given on the four stations with the strongest (in terms of PGA) motions (shown as filled triangles in the figure). The peak recorded acceleration inside the Syntagma station is reported in Fig. 1 only for completeness; no analyses for this station are presented in this article. With the exception of five records, all others were

recorded at structures related with the just-constructed Athens Metro. The three strongest recorded accelerograms and their elastic response spectra ( $\zeta = 5\%$ ) are presented in Fig. 2. The first two of these accelerograms were recorded on the ground surface, and are utilized in determining the base motion at the sites of Monastiraki and Sepolia, respectively, through an inverse analysis procedure (deconvolution). The ‘rock-outcrop’ KEDE record will be used as the base excitation for the analysis of the Kerameikos retaining system, since it is located at a distance of less than 1 km from that site.

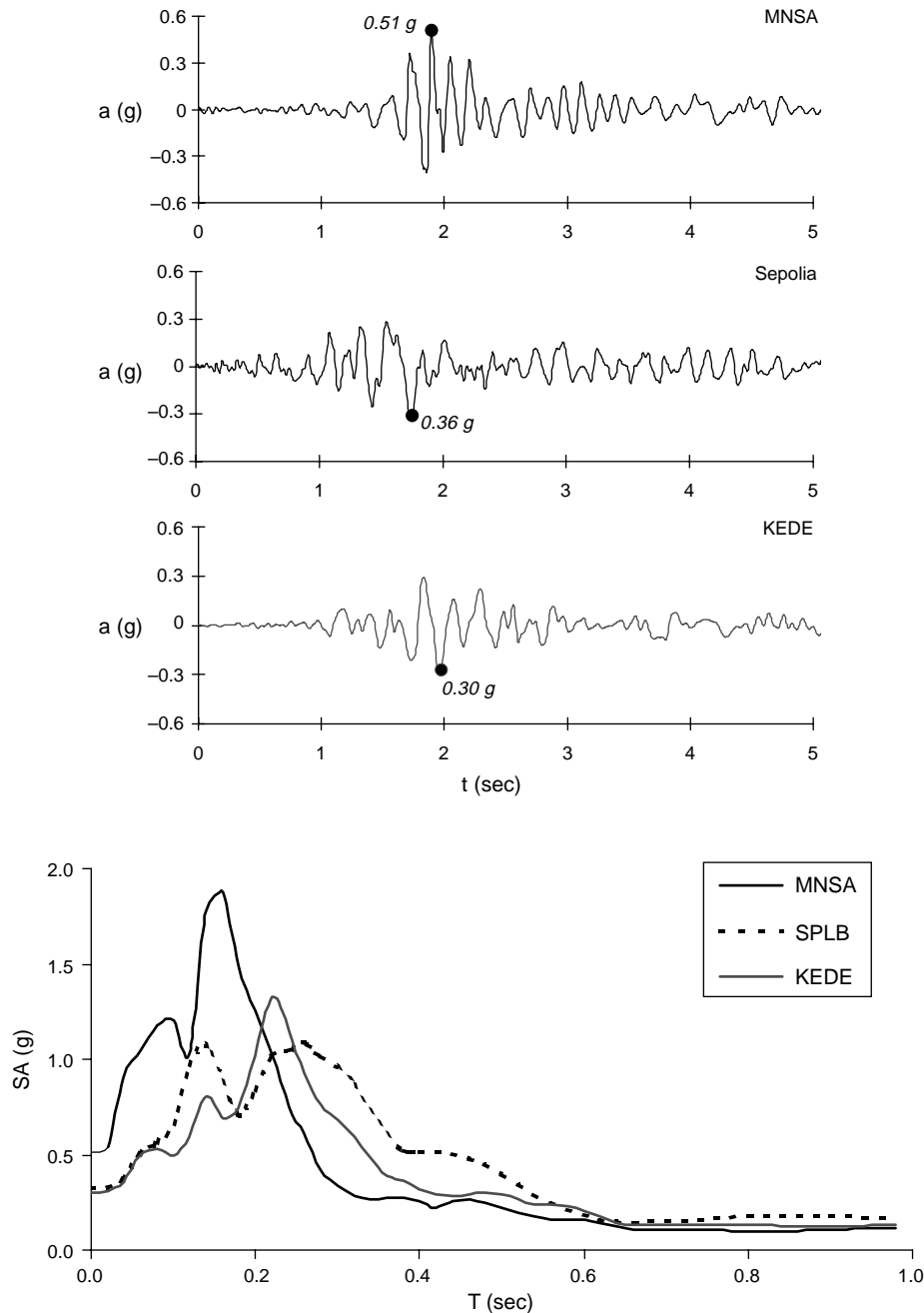


Fig. 2. The three strongest records of the Parnitha 1999 earthquake and their response spectra (MNSA, Monastiraki acceleration; SPLB, Sepolia acceleration station; KEDE, KEDE station).

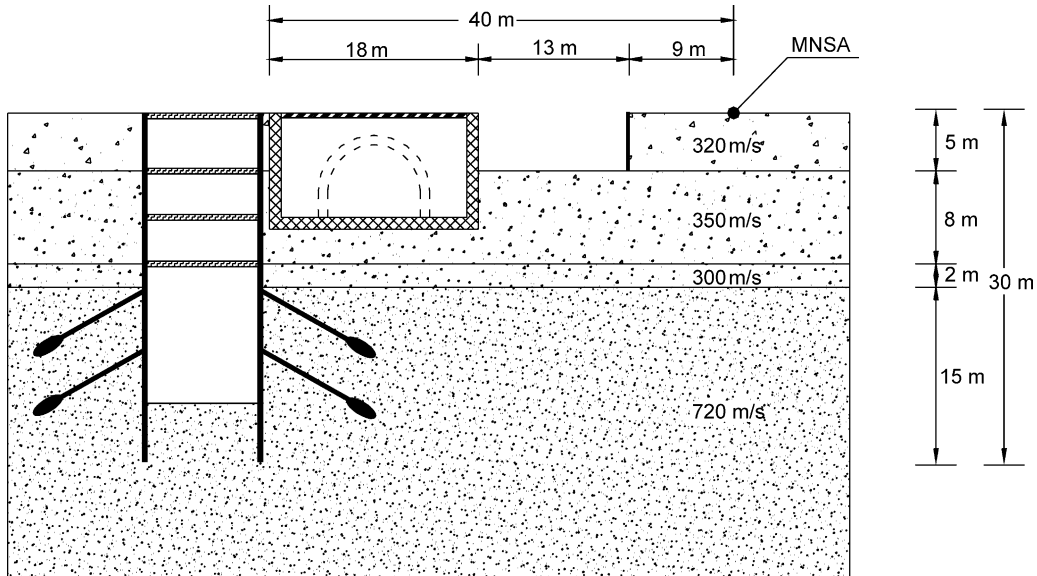


Fig. 3. Vertical section through the Monastiraki seismographic station (MNSA), showing the temporary support of the excavated shaft, the walls of the existing metro-line and the adjacent excavation for archaeological search.

### 3. The Monastiraki station

The accelerograph station at Monastiraki (MNSA) recorded a very high PGA, 0.51 g, in one direction. The very low dominant periods that characterize this record (from 0.08 to 0.17 s) could only partly explain the small degree of building damage in the neighbourhood of

the station in spite of spectral accelerations exceeding 1.50 g. However, having been recorded next to a deep shaft of an under-construction Metro station, this accelerogram aroused suspicion that it might have been affected by the underground structure. Indeed, in addition to the shaft, two other underground ‘structures’ were present very close to the position of the instrument. As shown in Fig. 3,

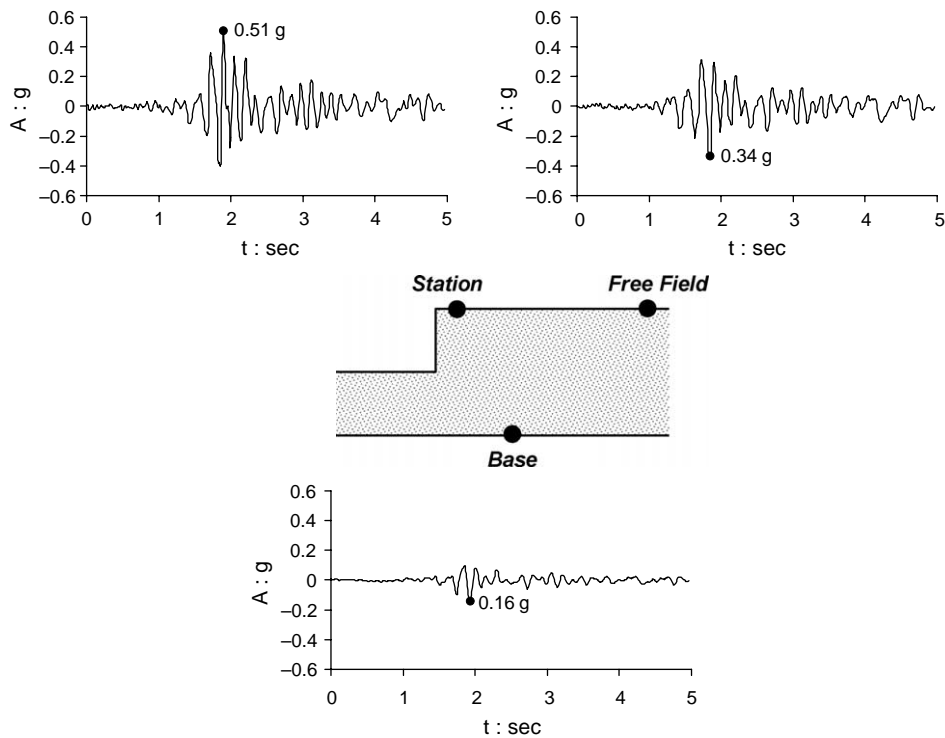


Fig. 4. Results of the 2D deconvolution for Monastiraki: upper left: the recorded motion, bottom: the motion obtained from 2D deconvolution, and upper right: the computed free-field motion (from [5]).

in a vertical plane section almost parallel to the strongest component of the motion, a heavy-walled shallow tunnel of the old metro line (18 m wide and 10 m deep) and a 5-m-deep open archaeological excavation pit lie between the instrument position and the shaft. The soil profile comprises stiff sandy clays and highly weathered rock formations down to at least 60 m depth. The weighted average value of velocity at depths  $z \leq 30$  m is about 400 m/s—category C according to the NEHRP 1997 Provisions [4].

An *inverse* procedure was implemented, using finite-element modelling of the ‘structure’, with the record under investigation being the ‘target’ surface motion. Equivalent-linear soil properties were assigned to the soil elements, with the assumption of vertical S wave propagation. One-dimensional (1D) equivalent-linear wave-propagation analyses were thus performed utilizing well established empirical curves for the decrease of shear modulus and the increase of material damping with increasing amplitude of shear strain for each soil layer. Then, two-dimensional (2D) wave propagation analyses were conducted using

strain-compatible (equivalent) soil parameters obtained from the 1D analysis.

The results of the inverse analysis procedure (from [5]) are presented in Fig. 4. They confirm that the presence of the three underground structures has indeed spuriously enhanced the acceleration amplitudes in one of the horizontal components of the instrument. Wave diffraction at the corners has apparently led to an increase of about 30% in peak ground acceleration compared to what would have been recorded in a truly free-field. The motion recorded at the accelerograph station (PGA 0.51 g): (i) could be numerically derived from a base (–60 m) motion of  $\text{PGA} \approx 0.16$  g, and (ii) is consistent with free-field ground-surface acceleration amplitudes of  $\text{PGA} \approx 0.34$  g. The latter value is in better agreement with the peak values of the neighbouring stations (KEDE 0.30 g and SYNTAGMA 0.25 g). Evidently, both *soil flexibility* and *underground ‘obstacles’* have had their imprint (one-dimensionally and two-dimensionally) on the record.

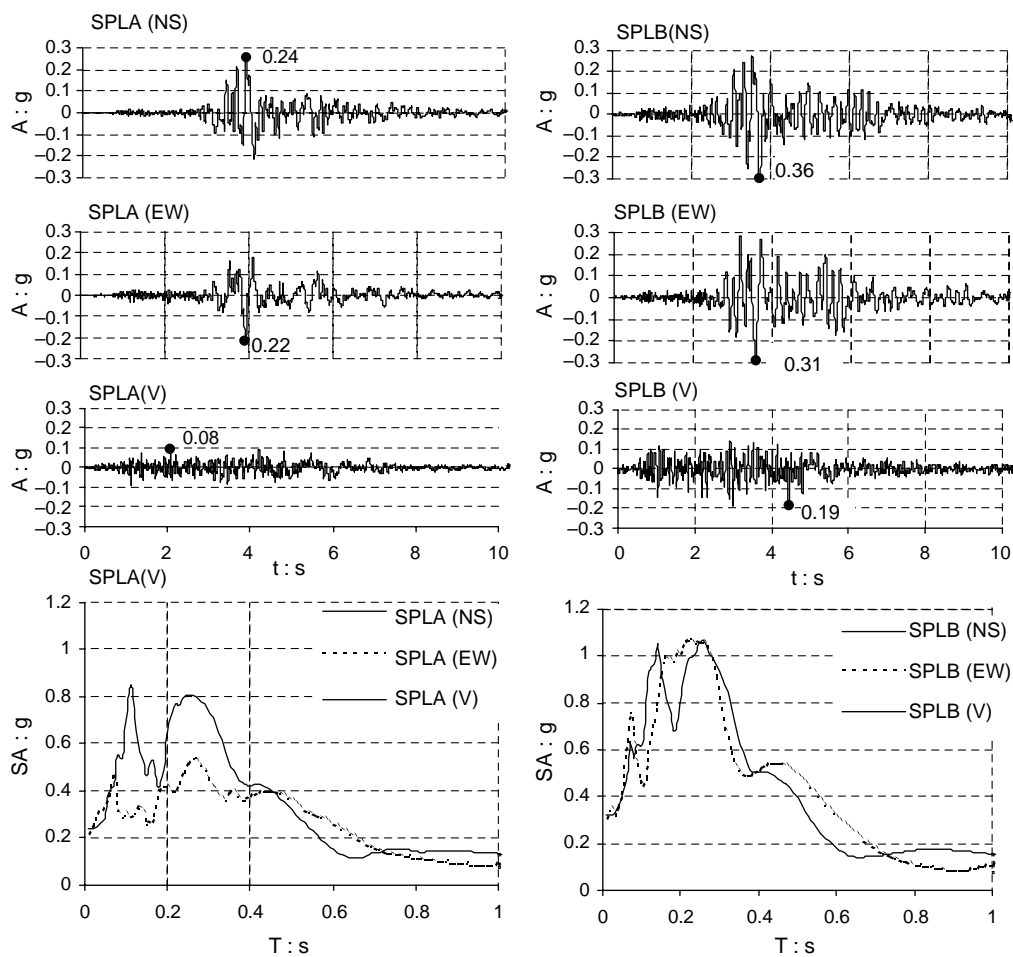


Fig. 5. The two records at Sepolia station with the corresponding response spectra. Left, the motion inside the station at a lower level; Right, the motion on the surface of the free-field.

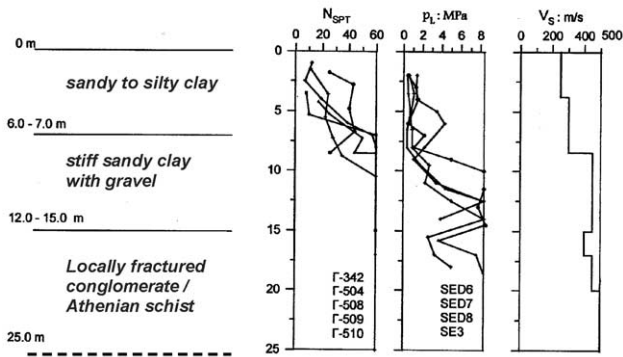


Fig. 6. Typical soil profile for the Sepolia station, with the measured values of the SPT, the pressuremeter test, and the seismic downhole tests.

**4. The Sepolia station**

Two accelerographs had been installed in the area of the Sepolia station, one inside the station at 12.9 m depth (SPLA), and another one (SPLB) approximately 500 m away from the station, practically in free-field. The recorded motions as well as their elastic response spectra are

presented in Fig. 5. SPLB has the longest period of ‘strong shaking’ among all the 13 recorded accelerograms. Its two horizontal components have practically the same PGA ( $\approx 0.31$  g) and their response spectra exhibit higher spectral accelerations in the long period range than all other records of the Parnitha earthquake:  $SA \approx 1.0$  g for periods ranging from 0.18 to 0.30 s, and  $SA \approx 0.50$  g for periods around 0.50 s. SPLA is characterized by lower PGA  $\approx 0.23$  g, while at the same time its frequency content is different. Observe, that its longitudinal component (SPLAL), which is parallel to the station axis, exhibits higher spectral accelerations for periods between 0.10 and 0.35 s.

As for all metro stations, detailed geotechnical investigation had been performed for the Sepolia station, comprising borings, pressuremeter testing, laboratory testing, SPT loggings, and Crosshole  $V_s$  measurements. Although the acquired experience from the construction of the Athens Metro suggests that soil conditions are generally very heterogeneous, a typical soil profile for the Sepolia station is presented in Fig. 6. The first 6–7 m comprise layers of sandy to silty clay, followed by a 6–8 m deep layer of stiff sandy clay with gravels, while at

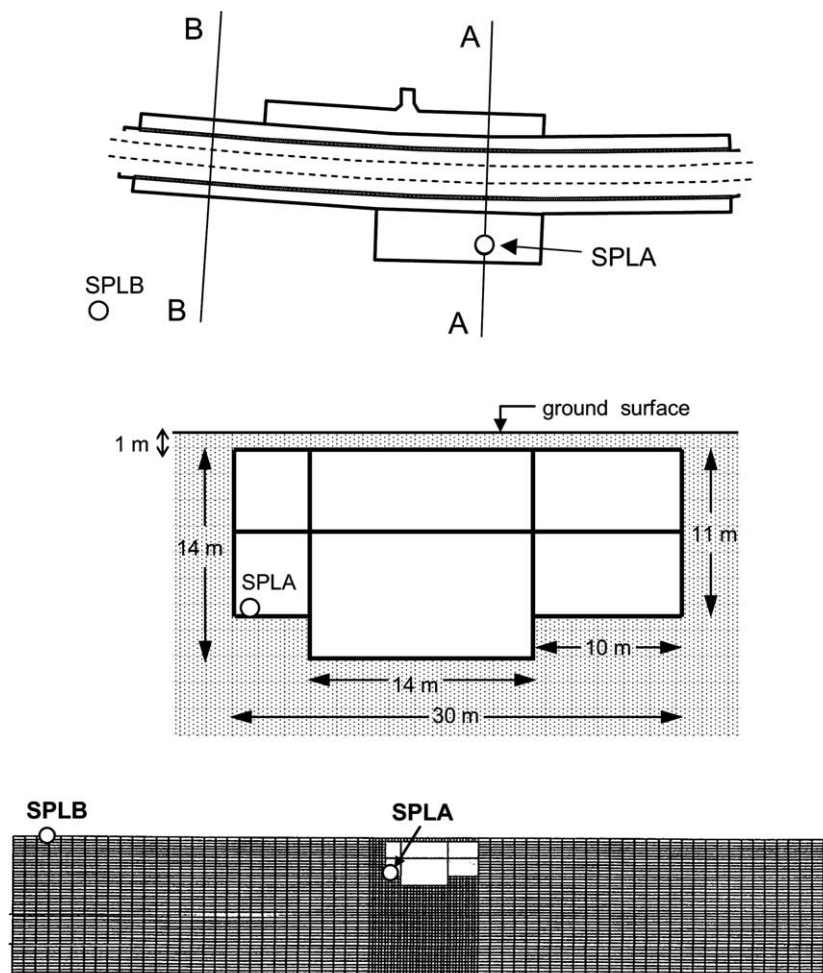


Fig. 7. Plan, cross section, and finite element discretization for the Sepolia station (Section A–A) and location of the accelerographs.

a depth of 12–15 m a locally fractured conglomerate exists, followed by ‘Athenian Schist’.  $N_{SPT}$ , pressuremeter stress  $p_L$ , and  $V_s$  measurements are qualitatively consistent.

A 2D *inverse* method, similar to the one used for the analysis of the Monastiraki station, is performed, as schematically illustrated in Figs. 7 and 8. Since in this case, a free-field record was available (SPLB), the 1D deconvolution was performed directly, in one step, to derive the ‘rock-outcrop’ motion. This motion was then utilised to describe the base excitation of the two-dimensional finite-element model. The validity of the analysis is controlled through the comparison between the recorded accelerogram inside the station (SPLA), with the calculated one.

This comparison is performed both *qualitatively* (i.e. direct ‘visual’ comparison of recorded and computed accelerograms) and *quantitatively* (i.e. through the ratio of corresponding Fourier amplitude spectra). Indeed, observe in Fig. 8 that this ratio undulates around unity, and only at very small and very large frequencies ( $\approx 0.25$  and  $\approx 4.5$  Hz, respectively), does it reach values of about 1.50. This is clearly a very satisfactory agreement of recorded and computed motions. Again, as for Monastiraki, the two-dimensional modelling is based on the equivalent linear soil behaviour. To avoid possible inaccuracies caused by the inherent imperfection of the so-called *free-field* boundaries, the latter were placed as far as (computationally) possible from the station.

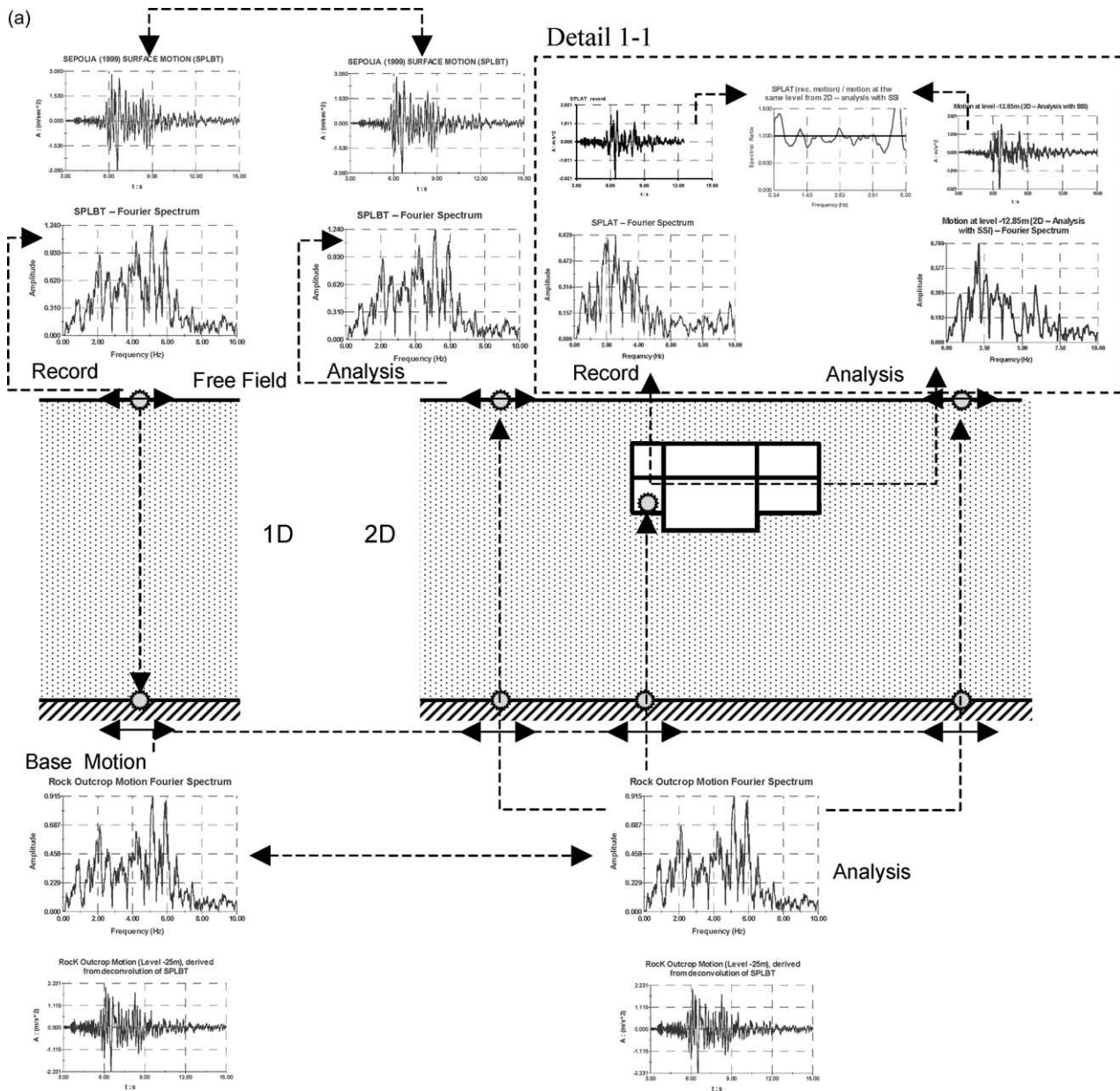


Fig. 8. (a) Explanation of the methodology for seismic response analysis of the Sepolia station (Section A–A) utilising the recorded accelerograms. (b) Enlargement of the detail 1-1 (a): Fourier spectral ratio of the recorded (target) and the computed accelerograms.

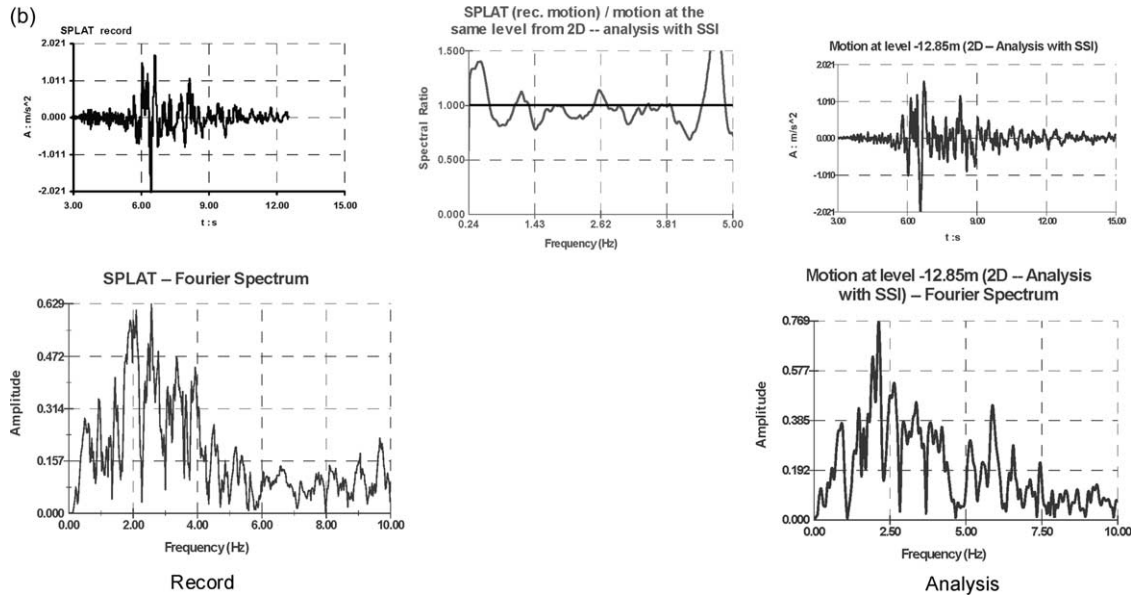


Fig. 8 (continued)

Fig. 9 presents the computed acceleration time histories, and Fig. 10 the time histories of bending moments at various key points of the walls of the structure. These results indicate that the Sepolia station was fairly severely shaken during the 1999 earthquake. The acceleration at the ‘roof’ of the station (just a meter below the ground surface) reached 0.45 g, while at its base it reached about 0.19 g. It is interesting to note that the computed accelerations are almost exactly equal to the design accelerations of the then

applicable Greek seismic code (NEAK): 0.46 and 0.184 g, for the roof and the base of the station, respectively. They correspond to the effective ground (base) acceleration  $A \approx 0.16 \times 1.15 \approx 0.184$  g, where 1.15 is the ‘importance factor’ that multiplies the zone acceleration of 0.16 g to give the design base acceleration. During design, the station was assumed to behave as an aboveground structure, and hence its roof acceleration was equal to  $S_a = 2.50 \times A = 0.46$  g, given its natural period of about 0.40 s. The fact that it

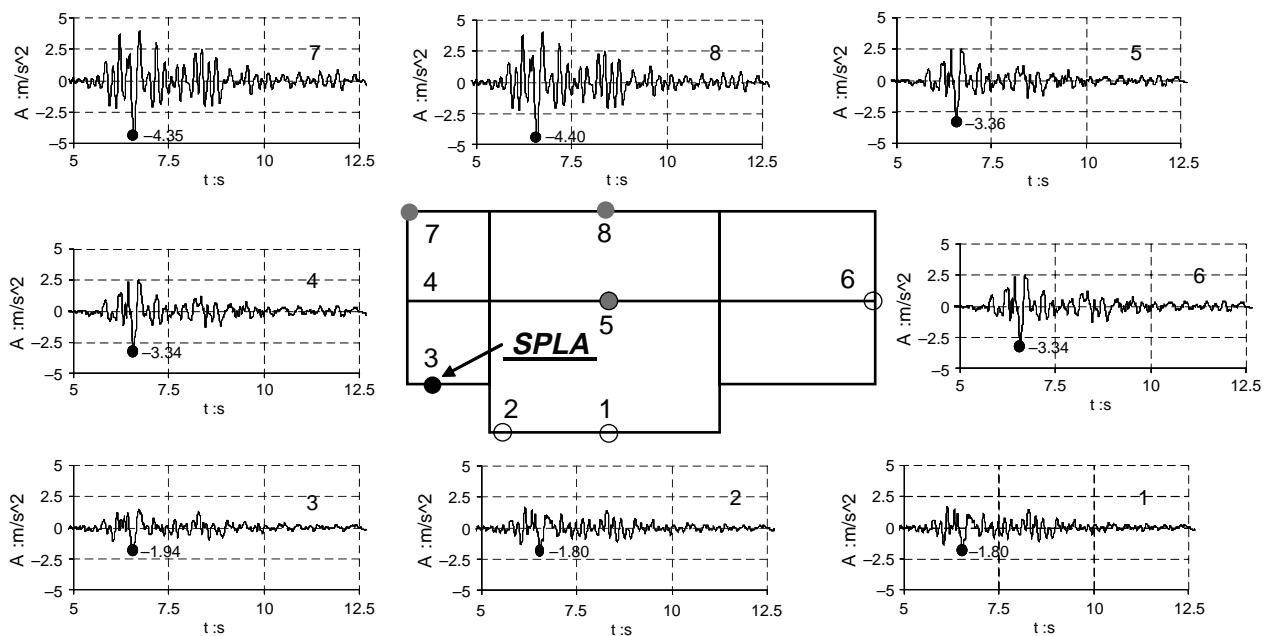


Fig. 9. Results of analysis for the Sepolia station (Section A–A): acceleration time histories at selected locations.



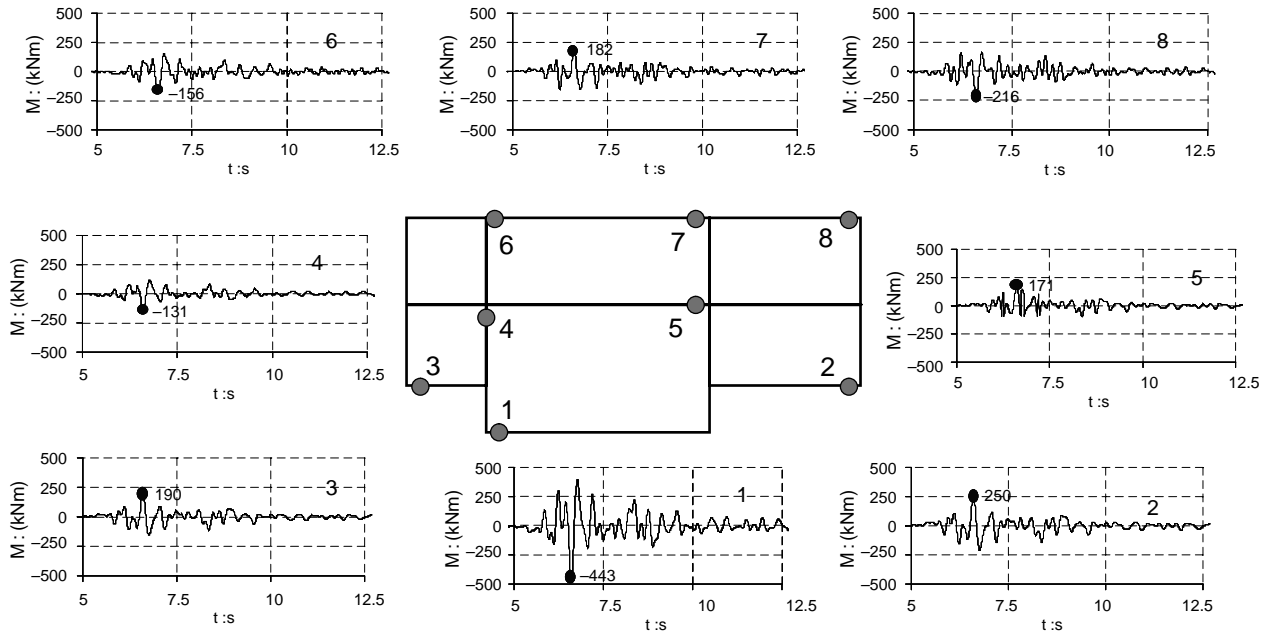


Fig. 10. Results of analysis for the Sepolia station (Section A–A): bending moment time histories at selected locations.

developed almost precisely these accelerations is partly a coincidence: the ground responded almost in unison with the structure, since it had a nearly identical strain-compatible fundamental period (about 0.35 s). One should therefore, be careful not to over-generalize this conclusion.

Despite the significant accelerations experienced at the top of the station, the developed dynamic internal forces are significantly lower than the capacity of the structure. For example, the maximum developed dynamic bending moment is found to be of the order of 300 kNm/m. This (additional) dynamic bending moment is found to be less than 1/3 of the static-design ultimate moment (computed for an 80 cm thick wall), and certainly much less than the *actual* bending capacity, leaving a significant margin of safety against plastic hinging. It is worth mentioning here that the structures of the Athens metro have been ‘capacity designed’ in accordance with the Greek Seismic Code. Thus, a possible failure would be flexural (exceedance of the yield bending moment and ductility capacity of the sections) rather than shear (insufficiency of transversal reinforcement). In addition, the calculated imposed shear forces are disproportionately lower than the shear capacity of the structural members of the stations. (These forces are not presented in this article.) Furthermore, note that even if a section were to plastify, the structure would not immediately become a mechanism. So, the inherent factor of safety of this conservatively designed structure against collapse is estimated to be of the order of 4.

To further assess the role of soil–structure interaction, the seismic response of a typical one-bay cross section of the Sepolia station, section bb, was analysed using the deconvoluted SPLB accelerogram as the seismic excitation at the base of the two-dimensional finite-element model.

A set of characteristic results is presented in Figs. 11–13. Specifically:

Fig. 11 portrays the distribution of the peak shear stresses and strains along the vertical walls. Comparison of the free-field peak shear stresses and strains with those acting on the tunnel wall (which obviously accounts for the soil–tunnel interaction [STI]), show that the interaction of the two media is not significant. Similar diagrams for the peak values of free-field and STI shear stresses and strains are presented in Fig. 12 for the base and the roof of the tunnel, respectively. One can notice that on the average, the shear stresses on the roof and the base of the station are about the same as the free-field stresses on a horizontal plane at the depth of the roof and the base, respectively. However, on the tunnel surfaces the stress are non-uniformly distributed: the maximum values occur in the middle of each surface.

Comparisons between peak shear and horizontal normal stresses and strains along the vertical walls of the tunnel are given in Fig. 13. A very interesting conclusion is derived from this figure. The seismic horizontal normal stresses (pressures) at the soil–wall interface are relatively small almost along the entire depth of the wall. This behaviour is similar to the response of a flexible retaining wall, as it will be shown in the following section, and is attributed to the fact that the embedded cut-and-cover box follows the ground motion without being significantly stressed (recall the similarity of natural periods of tunnel and soil deposit). It is also worth noticing in this figure that peak normal stresses become larger than the corresponding shear stresses only at specific points, where the rigidity of the structure is large. These points are the joints of the frame wall edge, party-wall edge and base-wall edge.

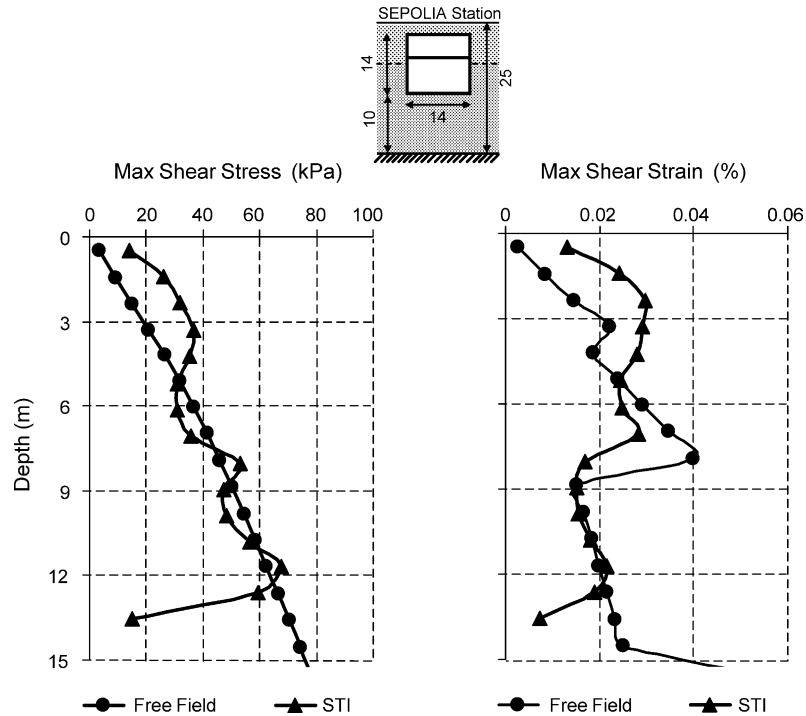


Fig. 11. Results of analysis for the Sepolia station (Section B–B): peak vertical shear stresses and strains developing along the vertical walls.

Comparing the seismic response of Sepolia station to that of Daikai station which failed in the Kobe 1995 earthquake [8,9], some interesting conclusions can be drawn:

- Daikai station suffered severe seismic loading with PGA values in the order of at least 0.70 g and spectral content rich in high-period components ( $T \approx 1\text{--}1.5$  s), compared with the weaker seismic loading of Sepolia station (PGA values of about 0.40 g and low period predominant acceleration components ( $T \approx 0.20\text{--}0.35$  s)).
- The soil surrounding Daikai station consisted of alternations of mostly saturated loose sandy and soft clayey layers with corrected SPT  $N_{60}$  values less than 20 [8]. The soils in Sepolia station had SPT values from 15 to 50 and the water table was 8 m below the ground surface. Soil deformations were evidently much larger in the Daikai station, imposing significant kinematic structural distress which was not the case in Sepolia.
- The collapse of the Daikai station might also be partially attributed to the destructive contribution of the 4.8 m thick overburden soil [8,9], the inertial force of which imposed significant roof distress (of the order of magnitude of the [high] frictional capacity of the soil–roof interface). This was not the case for the Sepolia station, where the overburden was only 1 m thick and the accelerations were not large enough to mobilize even the small frictional capacity of the soil–roof interface.
- The design of the Daikai station central columns was not according to modern capacity design method. The collapse mechanism involved the brittle failure of these columns due to combined shear, normal and moment

loading. (By contrast, the modern design of the Sepolia station followed capacity design principles which would ensure a ductile a bending failure mechanism, at much higher acceleration levels than those experienced in the 1999 Earthquake.)

To investigate the validity of simplified pseudo-static methods that only crudely reflect soil–tunnel interaction (STI), the computed dynamic earth pressures of Fig. 13 are compared with those proposed by the Greek Regulatory Guide [10] for the seismic analysis of bridge abutments. The aforementioned Guide (following similar AASHTO guidelines) proposes the following expression for the calculation of the average dynamic earth pressure:

$$\sigma_{\text{dyn}} = \lambda \alpha_0 \gamma H \quad (1)$$

where  $\alpha_0 (=A_0/g)$  is the peak ground acceleration (presumed to be unique in space),  $\gamma$  is the unit weight of the soil, and  $\lambda$  is a coefficient depending on the ratio between the expected (or allowable) displacement at the top of the wall  $U$  to its height  $H$ :

$$\lambda = \lambda(U/H) \quad (2)$$

For flexible walls ( $U/H > 0.10\%$ ),  $\lambda$  is taken equal to 0.375 in accordance with Mononobe–Okabe as interpreted by Seed and Whitman [11]. In the case of perfectly rigid and immovable walls ( $U/H < 0.05\%$ ),  $\lambda$  is equal to 1, while for intermediate cases  $\lambda$  is taken equal to 0.75 in broad agreement with Veletsos and Younan [12,13].

To evaluate the above method, Fig. 14 portrays the calculated acceleration and displacement time histories at

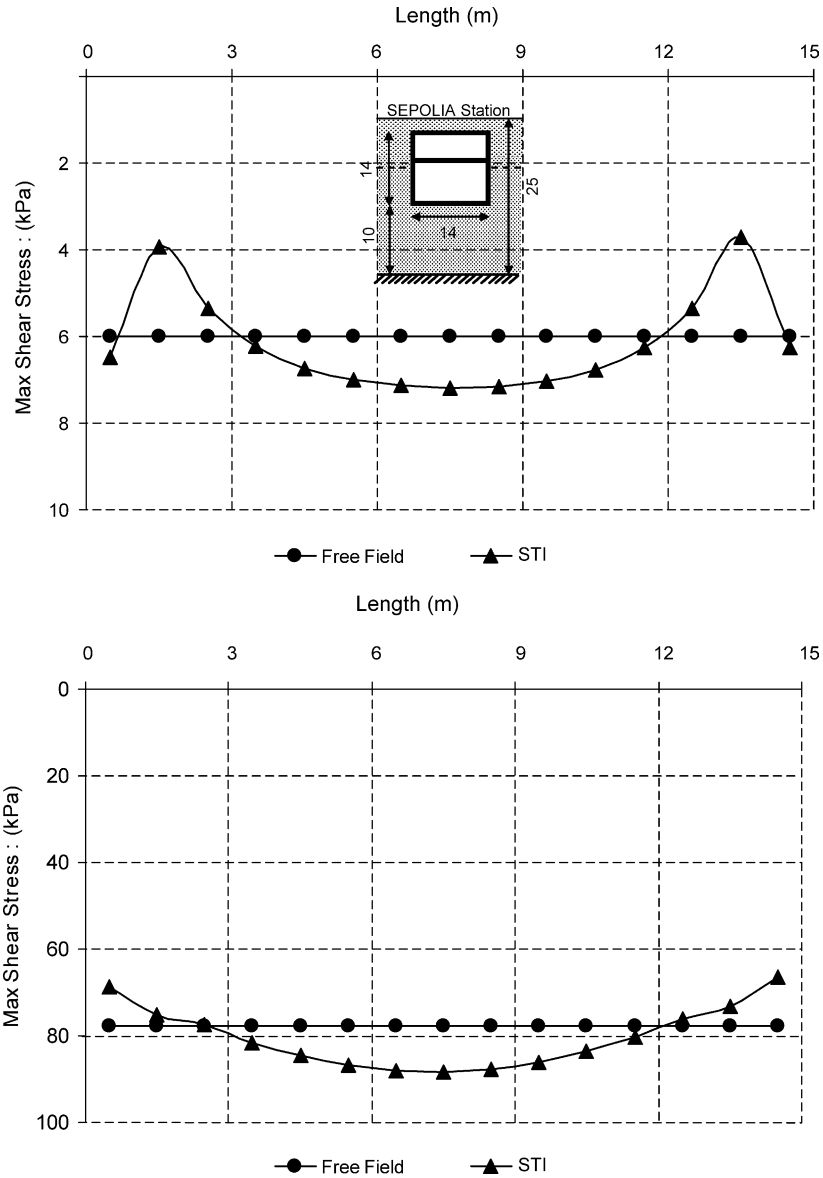


Fig. 12. Results of analysis for the Sepolia station (Section B–B): peak shear stress distributions along the roof (top), and the base (bottom).

the top and the base of the Sepolia station (Section B–B). The peak acceleration of the roof reached 0.43 g, while that of the base 0.17 g. The relative dynamic displacement of the station top, with respect to its base is calculated to about 0.7 cm or 0.05% of the wall height. Thus, considering  $a_0g$  as the average peak acceleration along the height of the station (a reasonable and unavoidable simplification)

$$a_0 \approx (0.17 + 0.43)/2 = 0.30 \quad (3a)$$

and for a unit weight for the soil  $\gamma \approx 20 \text{ kN/m}^3$ , the average dynamic earth pressure is calculated as:

$$\sigma_{\text{dyn}} = \lambda \alpha_0 \gamma H = 0.75 \times 0.30 \times 20 \times 14 \approx 63 \text{ kPa} \quad (3b)$$

As seen in Fig. 13, the above estimate exceeds the values calculated with our STI analysis, except along the lowest 4 m of the station. It will be seen in the results of the next

studied metro station (Kerameikos) that, indeed, simplified pseudo-static methods that ignore STI lead in general to conservative designs. Gazetas and co-workers [6,7] have further shown that this is usually the case with walls in stiff soils subjected to high-frequency excitation.

In conclusion, soil–tunnel interaction (STI) has been shown to have a small but noticeable effect on the response of the Sepolia station.

### 5. The temporary wall of the Kerameikos station

The excavation and installation of the temporary retaining system of the Kerameikos station started in the fall of 1995 and was completed in April 1996. At the end of the same year when construction of the permanent structure

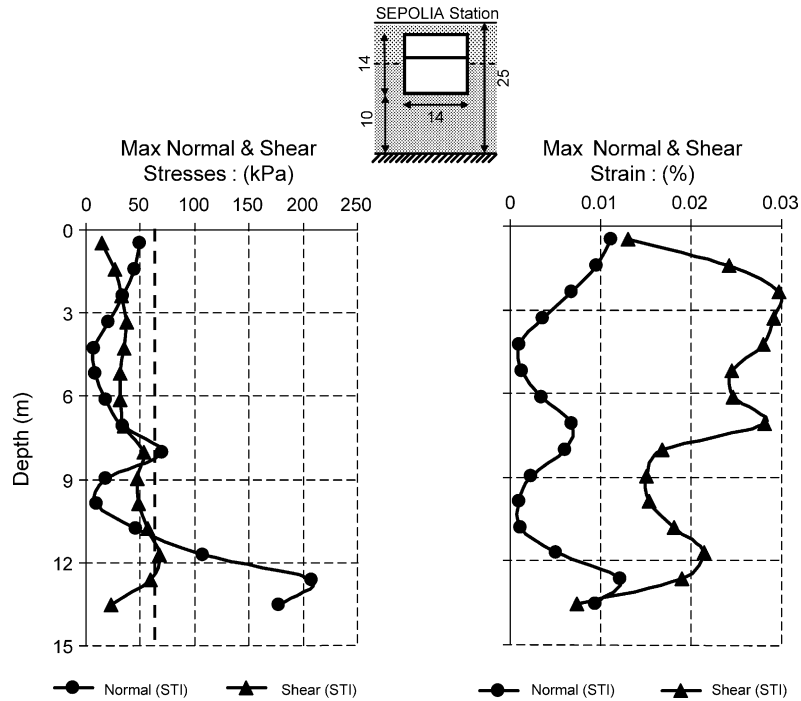


Fig. 13. Results of analysis for the Sepolia station (Section B–B): comparison of the peak values of the horizontal normal and vertical shear stresses and strains, developing along the vertical walls. The Mononobe–Okabe pressures, according to Refs. [10,11], are shown as dotted line.

had just started, the work was terminated for non-technical reasons, and the station was abandoned as such. At that time the excavation had reached 23 m with most of the related excavation works nearly completed. A photo and a sketch of the plan view of the abandoned station, are presented in Fig. 15. As shown in Fig. 16 (the inside part was never constructed, except for a small part of it), the retaining system comprised piles of 0.8 m in diameter, spaced at

1.8 m, and 15 cm thick shotcrete. Each pile was tied back with 5–7 anchors, of 12–24 m in total length, with the prestress load varying from 480 to 800 kN. The construction of the base slab of the station had also started immediately after excavation, but was left only half completed.

The soil profile is rather straightforward: 5–7 m of alluvium sand, followed by Athenian schist, fractured and weathered, with high degrees of heterogeneity.

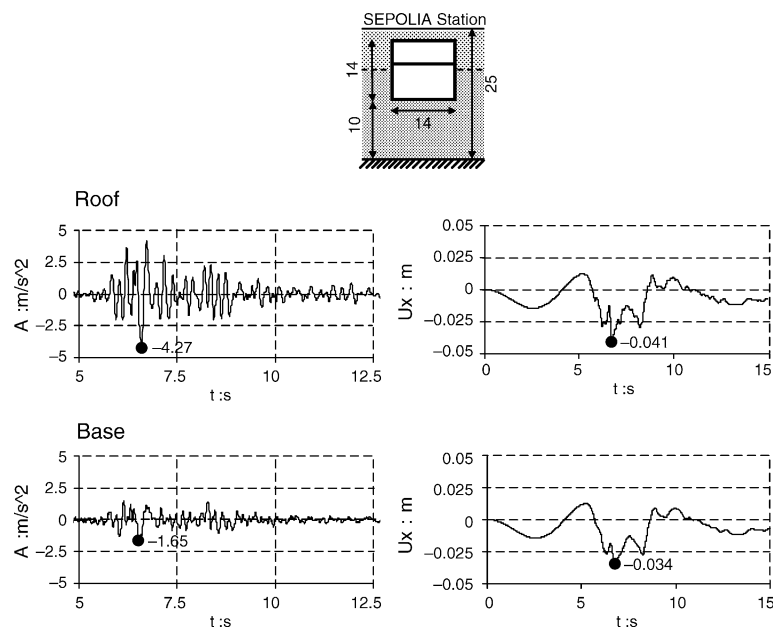


Fig. 14. Computed acceleration and displacement time histories for the roof and the base of the Sepolia station (Section B–B).

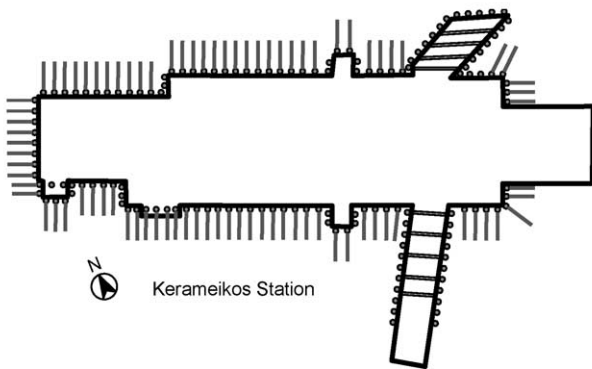


Fig. 15. A photo (top) and the plan (bottom) of the Kerameikos station (with the piles, the anchors, and the entrance-struts shown schematically).

During excavation and anchoring, a substantial horizontal outward displacement of the wall was recorded, reaching 9 cm (occurring at about 2/3 of its maximum depth, i.e. at  $\approx -15$  m). Although the retaining structure had not been designed against earthquake, since it was supposed to be only temporary, its performance during the 1999 earthquake (almost three years after its abandonment) was exceptional. The retaining structure survived the earthquake with no visible damage, other perhaps than a few small cracks at

the shotcrete, which could possibly have existed before the earthquake. No damage was observed in neighbouring structures, buildings, pavements, etc. which could be attributed to the shaking response of the retaining system. The wall did not show any additional permanent (plastic) deformation.

To explore the (surprising) success of this retaining structure the system was analysed numerically utilizing the FE method. The measured static performance of the system was utilized to calibrate the (effective) soil properties, which were then used to derive realistic dynamic parameters. The 2D linear analysis was based on the equivalent soil parameters obtained from the last iteration of a 1D equivalent-linear analysis. According to the above methodology, shear wave velocities of  $V_s = 135$  and 280 m/s were assigned, respectively, to the first 7 m of alluvium sand and the underlain 23 m thick soft Athenian schist. A 1D deconvolution was performed to derive the 'rock-outcrop' motion (as the base excitation), with the KEDE record scaled at a PGA of 0.50 g, as the target free-field surface motion. This was a somewhat conservative estimate of the level of acceleration. The KEDE motion was utilized only because it was recorded close to the site, at a distance of less than 1 km. Fig. 17 portrays the finite-element mesh and the computed acceleration time histories at two locations: at the top of the retaining wall, where PGA reaches 0.56 g, and at a distance of  $1.5H$  away from it, where PGA reaches 0.51 g. Observe that there is only one peak that reaches 0.51 g, with the rest of the record being well below 0.35 g. The slight difference of the PGA value of the first record (0.56 g) from that of the target free-field value (0.50 g), is attributed to the diffraction of waves from the vertical cut. The PGA value of the second record (0.51 g) is practically equal to the target free-field value, implying that at a distance of  $1.5H$  away from the retaining wall, the motion is not affected to any appreciable degree by the geometry of the excavation and the presence of the retaining system.

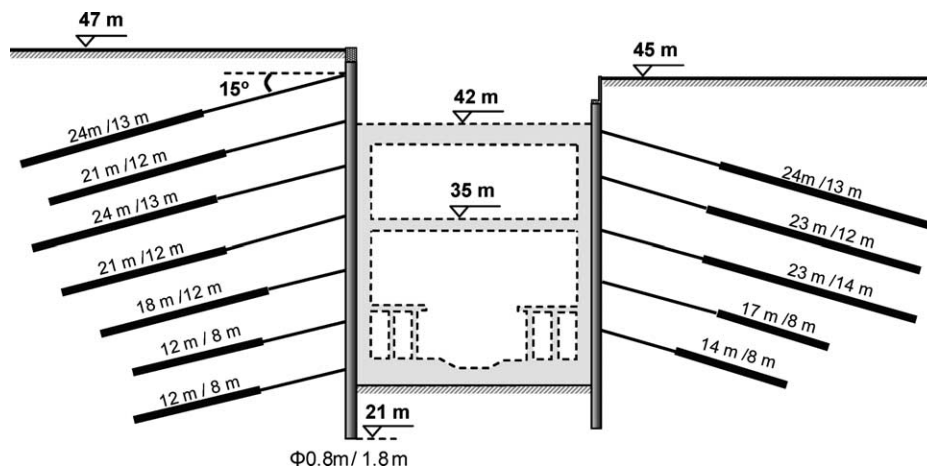


Fig. 16. Typical cross-section of the Kerameikos abandoned excavation. The inside grey of the part with dotted lines was never built, except for a very small part at one side of the excavation.

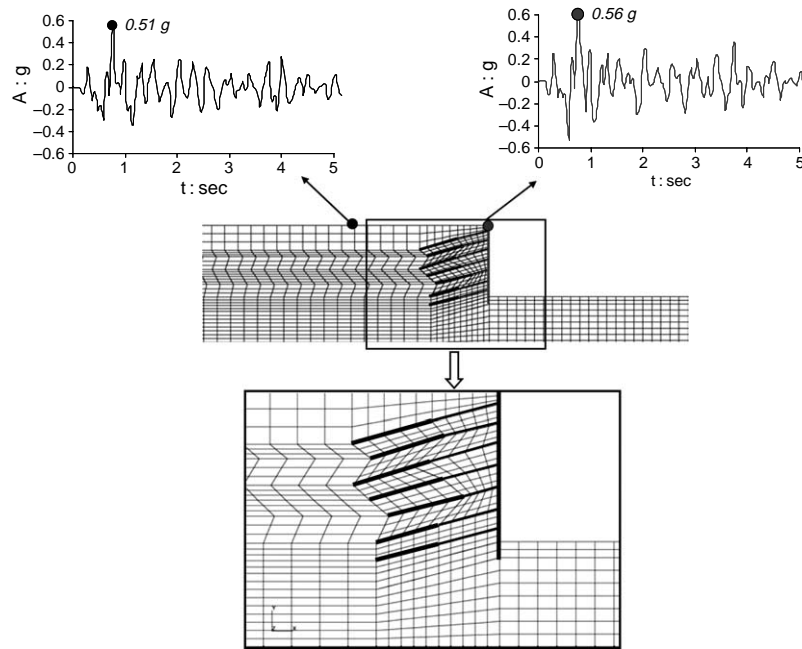


Fig. 17. Results of analysis for the Kerameikos station: finite-element discretization and acceleration time histories at two locations.

With the retaining structure being subjected to such high PGAs, one might have expected that damage would have been serious. In reality, no damage was observed. To explain this excellent behaviour, we refer to Fig. 18, where time histories of anchor forces are displayed. Surprisingly, all anchor axial dynamic forces are practically insignificant. In the worst case, the maximum anchor dynamic force reached merely 15 kN/m—a value of no significance, when compared to the static prestressing forces which ranged from 290 to 530 kN/m. This interesting conclusion is further reinforced with Fig. 19, where time histories of seismic

bending moments at selected points of the retaining wall are portrayed. Their amplitudes are indeed very small.

In Fig. 20, the distributions with depth of dynamic displacements and bending moments are also of interest. The maximum dynamic displacements are shown to reach 3.5 cm, while the maximum dynamic bending moment in the wall barely exceeds 120 kN/m. None of these two values is indicative of any serious distress of the retaining system. In fact, the 3.5 cm of dynamic displacement (i.e. a mere 0.1% of the wall height) would correspond to almost elastic soil behaviour, and indeed the measured residual

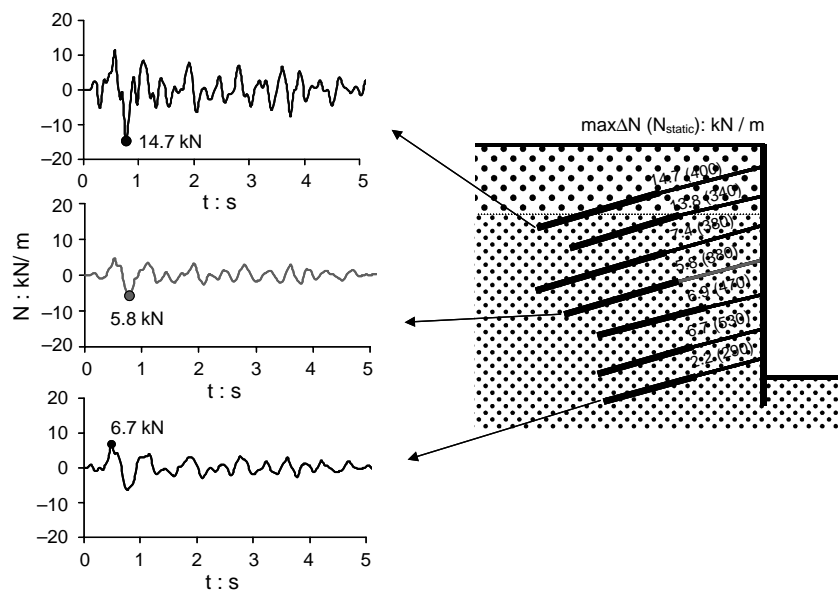


Fig. 18. Results of analysis for the Kerameikos station: selected anchor force time histories. Peak values of the dynamic anchor forces are compared with the respective static values (shown in parentheses).

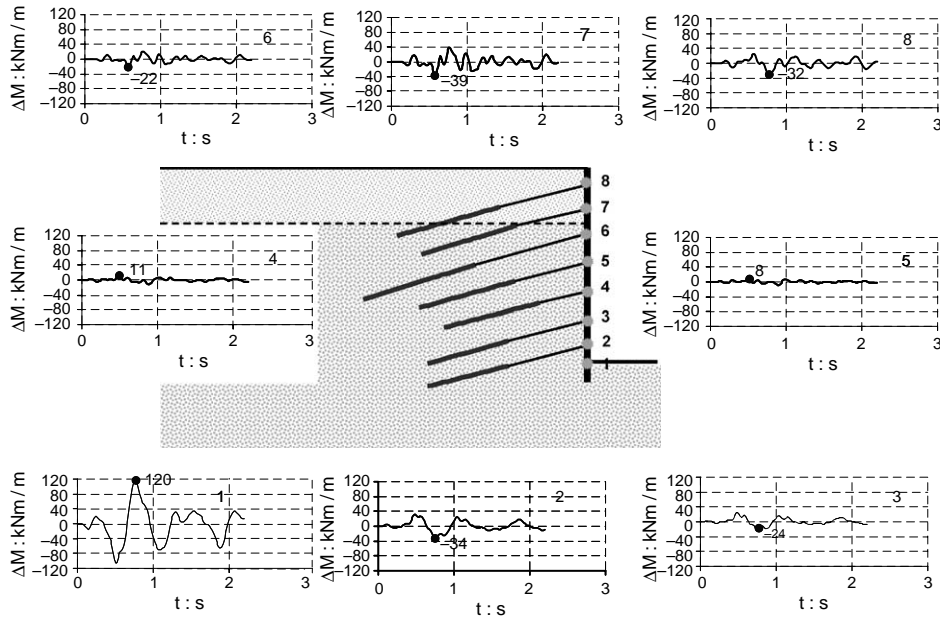


Fig. 19. Results of analysis for the Kerameikos station: bending moment time histories at selected points of the retaining wall.

displacement was measured even smaller (2.5 cm). Apparently, as it is shown in Fig. 21, thanks to its inherent flexibility relative to the stiff soil (backfill), the wall follows the ground motion without being significantly stressed. It is evident in this figure that the maximum seismic horizontal stresses at the soil–retaining wall interface are practically negligible almost along the entire depth of the wall. Two exceptions to this: (a) near the tip of the wall due to the presence of the base soil which acts as a restrainer to the movement of the wall, and (b) at the interface of the surficial soil layer and the underlain stiff one ( $\approx 7$  m). Although the anchors play a very significant role statically, under the specific dynamic conditions imposed by the 1999 earthquake, they simply follow the movement of the ground.

Certainly, the substantial stiffness and strength of the retained soil is one of factors influencing this favourable response of the anchors and the piled wall: if the soil were softer, a Coulomb-type wedge failure mechanism would have developed. Then, both normal earth pressures on the wall and axial forces in the anchors would have increased to levels roughly comparable to those predicted by the Mononobe–Okabe pseudostatic method of analysis [7].

The high-frequency content of the motion is another key factor for the success of the Kerameikos retaining wall. Had the excitation been richer in long periods, the structure would possibly have experienced some distress. This is in agreement with the conclusions drawn in [6,7] for a variety of flexible retaining structures.

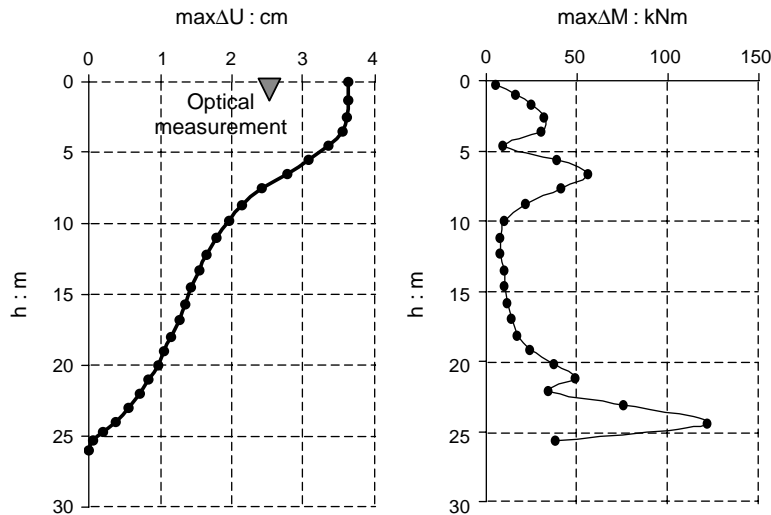


Fig. 20. Results of analysis for the Kerameikos station: distribution of the peak values of seismic displacement and bending moment of/in the retaining wall.

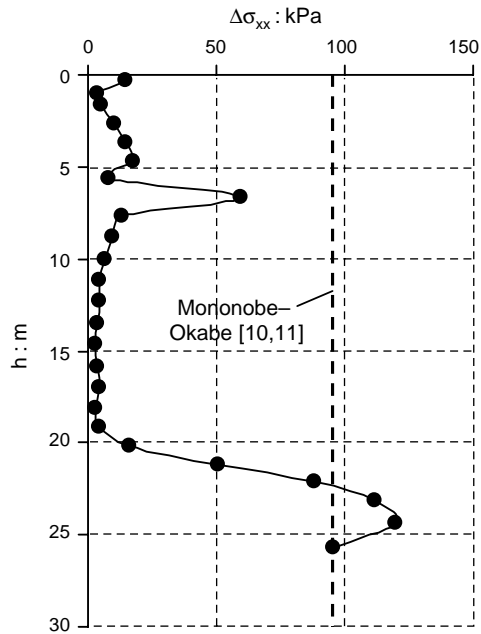


Fig. 21. Results of analysis for the Kerameikos station: peak values of the seismic horizontal stresses acting against the pile wall.

Calculating the average dynamic earth pressures according to Mononobe–Okabe [10,11], as described in Section 4, we find

$$\sigma_{\text{dyn}} = \lambda \alpha_0 \gamma H = 0.375 \times 0.45 \times 22 \times 25 \approx 92 \text{ kPa} \quad (4)$$

where 0.45 g is the average PGA value along the height of the wall, from our analysis. This value again overpredicts the average dynamic earth pressure calculated from the 2D analysis (Fig. 21) in which soil–structure interaction was fully accounted for.

## 6. Conclusions

The 1999 Athens (Parnitha) Earthquake offered valuable records of the seismic response of a number of subway stations and retaining structures of the Athens Metro. The article has presented some of these records with an attempt to analytically interpret their meaning. Some of the main conclusions of our study are as follows:

(a) In the case of the Monastiraki station the presence of three excavations is shown to have spuriously enhanced the acceleration amplitudes recorded on the ground surface. Wave diffraction at the corners of these excavations has led to an increase of about 30% in peak ground acceleration compared to that of the free-field. The recorded PGA, 0.51 g, could be numerically derived from a base (–60 m) motion of  $\text{PGA} \approx 0.16 \text{ g}$ , and was shown to be consistent with free-field ground-surface acceleration amplitudes of  $\approx 0.34 \text{ g}$ . The latter PGA value is in better agreement with the recorded

PGA in the neighbouring station of KEDE (0.30 g) and Syntagma (0.25 g).

- (b) The Sepolia station experienced the strongest shaking during the Parnitha earthquake. Using the free-field record and the record at the station second level, we have numerically demonstrated that: the accelerations induced from the earthquake, with  $\text{PGA} \approx 0.20 \text{ g}$  at the station base and 0.45 g at the station roof, are almost exactly equal to the design accelerations (according to the Greek seismic code). Nevertheless, despite this ‘design-level’ shaking, dynamic internal forces are significantly lower than the capacity of the structure. Evidently, soil–tunnel interaction has affected the response of the station. Modern design methods for cut-and-cover subway stations built in stiff soils lead to structures with ample margins against failure. Problems could only arise when much stronger shaking takes place, or softer/looser soils exist, or the station design is more vulnerable than the present-day reinforced concrete robust structures. Such adverse conditions apparently co-existed and caused the failure of the Daikai station in Kobe during the 1995 Earthquake [8,9].
- (c) The temporary prestressed-anchor piled wall of Kerameikos survived the earthquake with no visible damage. It is shown that the inherent flexibility of the wall leads to minimal dynamic earth pressures in this case of *stiff* retained soil. The maximum dynamic axial forces in the anchors are also of small magnitude even under strong seismic shaking. The success of this retaining structure is also partially attributable to the high-frequency content of the ground motion. We cannot exclude the possibility that (for an excitation stronger and richer in long periods, and softer surrounding soil) the structure might have possibly experienced more substantial distress.

## Acknowledgements

We greatly appreciate the financial support and the permission to publish this work by Attiko Metro S.A. The help by M. Benissi and M. Novack is kindly acknowledged.

## References

- [1] International society for the prevention and mitigation of natural hazards. Catastrophic Athens (Greece) earthquake of 7 September 1999: an unexpected event in a low seismicity region. Special issue of *Natural Hazards*, vol. 27(1–2) 2002, p. 1–199.
- [2] Rondianni Th, Mettos A, Galanakis D, Georgiou Ch. The Athens earthquake of September 7, 1999: its setting and effects. *Annales Geologiques des pays Helleniques*, 1e Serie, T. XXXVIII, Fasc. B; 2000, p. 131–44.
- [3] Gazetas G. Analytical and experimental estimation of the ground motions in the meizoseismal region of the Athens 7-9-99 earthquake. Research report, National Technical University, vol. 1–3; 2001.



- [4] Dobry R, Borcherd RD, Crouse CB, Idriss IM, Joyner WB, Martin GR, et al. New site coefficients and site classification system used in recent building seismic code provisions. *Earthquake Spectra* 2000;16(1).
- [5] Gazetas G, Kallou PV, Psarropoulos PN. Topography and soil effects in the  $M_s$  5.9 Parnitha (Athens) earthquake: the case of Adames. *Nat Hazards* 2002;27:133–69.
- [6] Anastasopoulos I, Gazetas G, Psarropoulos P. Flexible retaining walls: why they do not often fail in strong seismic shaking? Proceedings of the fib symposium on concrete structures in seismic regions, Athens 2003.
- [7] Gazetas G., Psarropoulos P., Anastasopoulos I., Gerolymos N. Seismic behaviour of flexible retaining systems to short-duration moderately strong excitation. *Soil Dyn Earthq Eng*; 24:537–50.
- [8] Iida H, Hiroto T, Yoshida N, Iwafuji M. Damage to Daikai subway station. *Soils Found* 1996;283–300 [Special issue].
- [9] Matsuda T, Samata S, Iwatate T. Seismic response analysis for a collapsed underground subway structure with intermediate columns. The 1995 Hyogoken–Nabu earthquake—investigation into damage to civil engineering structure. Japan: Japan Society of Civil Engineers; 1996 p. 277–85.
- [10] Ministry of Public Works. Regulatory guide E39/93 for the seismic analysis of bridges. Bull Tech Chamber Greece, Issue No. 2040, 1998.
- [11] Seed HB, Whitman RV. Design of earth retaining structures for dynamic loads. Proceedings of the specialty conference on lateral stresses in the ground and design of earth retaining structures, ASCE 1970. p. 103–47.
- [12] Veletsos AS, Younan AH. Dynamic response of cantilever retaining walls. *J Geotech Geoenviron Eng*, ASCE 1997;123:161–72.
- [13] Veletsos AS, Younan AH. Dynamic soil pressures on rigid vertical walls. *J Earthq Eng Struct Dyn*, New York 1994;23:275–301.